Determination of polybutadiene microstructures and styrene–butadiene copolymers composition by vibrational techniques combined with chemometric treatment

ARTICLE *in* VIBRATIONAL SPECTROSCOPY · JULY 2001

Impact Factor: 2 · DOI: 10.1016/S0924-2031(01)00111-4

2 AUTHORS:

Jean Guilment
Arkema
30 PUBLICATIONS **731** CITATIONS
SEE PROFILE

Liliane Bokobza
MINES ParisTech
123 PUBLICATIONS **2,857** CITATIONS
SEE PROFILE

ELSEVIER

Vibrational Spectroscopy 26 (2001) 133–149

VIBRATIONAL SPECTROSCOPY

www.elsevier.com/locate/vibspec

Determination of polybutadiene microstructures and styrene–butadiene copolymers composition by vibrational techniques combined with chemometric treatment

Jean Guilment[a], Liliane Bokobza[b,*]

[a]*Kodak European Research Laboratories, CRT 60.3, Chalon/Saône, France*

[b]*Laboratoire de Physico-Chimie Structurale et Macromoléculaire, ESPCI, 10 rue Vauquelin, 75231 Paris Cedex 05, France*

Received 6 July 2000; received in revised form 28 March 2001; accepted 18 April 2001

Abstract

Vibrational spectroscopy techniques have been used to study the polymer composition using only one technique at a time. In this paper, mid- and near-infrared (NIR) as well as Raman spectroscopies are combined with partial least squares (PLS) in order to determine the *cis*-, *trans*- and vinyl-configurations of polybutadienes as well as the composition of styrene–butadiene copolymers. A critical comparison of these techniques for the microstructure analysis will also be presented not only in terms of quantitative results but also in the way the samples can be analyzed and the spectra interpreted. Each of the techniques gives comparable results in terms of the precision of the models developed (limited to the precision of the reference method), but we can also see that the NIR spectroscopy is more reproducible in the short term due to the high signal to noise ratio obtained on the spectra. On the other hand, Raman excited in the NIR (FT-Raman) is the only technique which is free of sample preparation and handling allowing to get very good results in the long term.

Keywords: Polybutadiene; Microstructure; Infrared spectroscopy; Near-infrared spectroscopy; Raman spectroscopy; Partial least squares; Chemometrics; Quantitative prediction

1. Introduction

The polymerization of 1,3-butadiene gives rise to polymers containing 1,4-*cis*, 1,4-*trans*, or 1,2-vinyl structural units or a mixture of these. The 1,2-units may be isotactic, syndiotactic or atactic. Vibrational spectroscopy can be used for the quantitative analysis of the different chemical sequences constituting polymeric materials [1–5].

The microstructure of a polybutadiene (PB), determined by the content of the *cis*-, *trans*- and vinyl-configurations, is of peculiar importance since it influences a wide range of physical properties. PBs and styrene–butadiene copolymers being completely hydrocarboned systems, are difficult to analyze by chemical methods.

Spectroscopic techniques, such as infrared (IR) [6–9], Raman [10–12] and NMR [13–15] spectroscopies, were used to characterize the microstructure

* Corresponding author. Tel.: +33-140-79-45-15; fax: +33-140-79-46-86.
E-mail address: liliane.bokobza@espci.fr (L. Bokobza).

0924-2031/01/$ – see front matter
PII: S0924-2031(01)00111-4

of PBs and the composition of styrene–butadiene copolymers (SBR). A critical assessment and a systematic comparison of the major spectroscopic techniques including mid-infrared (MIR) and Raman as well as NMR for the microstructure determination of these polymers was reported by Frankland et al. [16]. The quantitative analysis was carried out by a standard evaluation based on measurements of absorbances at specific wavenumbers in MIR, areas of Raman bands and peak intensities in ^{1}H NMR and ^{13}C NMR spectra.

In the present work, in addition to a MIR and FT-Raman investigation, near-infrared (NIR) spectroscopy is used to develop a quantitative determination of the PB microstructure and copolymer compositions.

The use of high-energy spectra has become a very popular technique for multi-component analysis of solid samples. The usefulness of this technique is mainly attributed to its ability to rapidly and non-destructively analyze bulk materials without any sample preparation. On the other hand, the introduction of chemometric evaluation procedures has contributed to the tremendous expansion and the current state of popularity of NIR spectroscopy. The potential of this technique in polymer analysis as well as in polymer physics has already been demonstrated [17–20].

This work presents a vibrational analysis of PBs of various microstructures and of styrene–butadiene copolymers of various compositions. The spectroscopic measurements are combined with a chemometric data treatment to provide calibrations for the determination of the *cis*-, *trans*- and vinyl-configurations as well as for the styrene content. A discussion about the ease of use of the different techniques is also proposed along with the precision obtained in each case.

2. Experimental part

All the elastomers investigated were provided by Manufacture Française des Pneumatiques Michelin (Clermont-Ferrand, France). Experiments were carried out at room temperature on raw polymers (about 0.2 to several mm thick).

Mid-infrared spectra were obtained with a Bruker IFS 66 spectrometer using the horizontal-ATR (HATR) technique on a 45° ZnSe crystal, at 4 cm^{-1} resolution from 600 to 4000 cm^{-1} (17–2.5 μm). NIR spectra were recorded at 8 cm^{-1} resolution from 4500 to 10,000 cm^{-1} (2.2–1 μm) with a vector 22/*N* spectrometer from Bruker spectrospin. Measurements were made through a fiber optic bundle probe in transflectance mode using an InGaAs detector cooled by Peltier effect using the 4500–10,000 cm^{-1} spectral range. Alternatively, an integrating sphere module (PbS detector with linearity correction) was used to collect the NIR radiation reflected from the samples (range 4000–10,000 cm^{-1}).

The Raman spectra were collected by retrodiffusion (180° configuration) in the 100–3500 cm^{-1} range at 4 cm^{-1} resolution under Nd-YAG laser illumination at 1.064 μm, 250 mW (advanced design lasers ADLAS 300) with a Bruker FRA 106 module attached to the IFS 66 spectrometer.

Each sample was measured three times with each technique to take into account the instrument variations. The MIR and Raman spectra are the result of the coaddition of 128 scans, while 64 scans were coadded to obtain each NIR spectrum. The calibration methods were developed using partial least squares (PLS) regression available on OPUS 'QUANT2' software from Bruker spectrospin.

3. Methods of investigation

3.1. Spectroscopic techniques

Mid-infrared spectroscopy, which gives access to fundamental vibrations, usually provides powerful information both on the concentration and chemical composition of the investigated system.

One practical problem in this range arises from the requirement of band absorbance which should roughly be lower than 0.7 optical density (OD) units in order to permit use of the Beer–Lambert law; absorbances appreciably higher can only be used with great care. That implies use of films sufficiently thin to be suitable for measurements in the normal transmission method. Depending on the extinction coefficient of the considered band, the required thickness can range from 1 to 200 μm. From this point of view, polymers with strong absorption bands are difficult to study.

The attenuated total reflection (ATR) technique is particularly useful for highly-absorbing materials. It is

based on the collection of the evanescent wave running along the polymer/crystal interface. The polymer is applied on the crystal by a pressing device, so that the contact area between polymer and crystal can be finely adjusted: the greater the contact area, the stronger the evanescent wave interacts with the sample. This technique allows collection of spectra from thick samples, providing that the pressure on the polymer is adjusted each time so that the Beer–Lambert law can be used for the following calculations and calibrations (absorbance in the 0.7 OD region). The light penetration in the sample being dependent on its wavelength, a Kubelka–Munk correction can be applied to obtain absorbance-like spectra.

An alternative method for obtaining vibrational spectra is by Raman spectroscopy. While a vibration is IR active if the dipole moment changes during the vibration, it is Raman active if the polarizability changes during the vibration.

The incoming laser beam is both reflected and scattered by the sample, and the Raman spectra are obtained by collecting the laterally diffused light. The technique is therefore well suited for thick samples, because the intensity of the collected light is much weaker than the reflected or transmitted one and is proportional to the analyzed volume.

One of the major drawbacks of Raman spectroscopy is the fluorescence which could arise from impurities, additives or thermal degradation of the samples. The fluorescence emission is highly dependent on the wavelength of the laser and is almost eliminated with FT-Raman where the excitation is located in the NIR region (1.064 μm) [21,22].

The analysis of thick samples can also be overcome by using NIR spectroscopy which examines overtones and combination bands much weaker than the fundamental modes. From this point of view, sample preparation is considerably simplified.

The NIR region of the spectrum covers the interval from about 12,500–4000 cm^{-1} (800–2500 nm). The bands in the NIR are primarily overtones and combinations of the fundamental absorbances found in the classical MIR region [23–25]. These absorption bands correspond mainly to vibrations of hydrogen-containing groups such as C–H, N–H and O–H. As these bands are much weaker than the corresponding fundamental absorptions, the principal advantage of NIR analysis is the ability to examine specimens several millimeters thick. In other words, the NIR region, which complements the MIR region, is analytically useful for spectroscopic applications involving analysis of samples containing very strong MIR absorbers. The key quantity in NIR spectroscopy is anharmonicity, which determines the occurrence and the spectral properties (frequency, intensity) of the NIR absorption bands [26].

Another problem occurring in the MIR spectra of rubbers arises from some absorptions of the ingredients of formulation. These absorptions, which 'spoil' the MIR spectra, vanish in the NIR region. Consequently, measurements carried out in the NIR range are more accurate than those obtained in the MIR region.

3.2. Chemometric data treatment

The emergence of statistical methods, essentially used for the treatment of NIR spectra, has allowed qualitative and quantitative information to be obtained from NIR absorptions which often are broad bands resulting from the overlap of many individual peaks. Additionally, the presence of Fermi resonances can also increase the complexity of the NIR spectra. A chemometric data evaluation is particularly useful for the analysis of PBs which contain C–H and CH_2 groups. Owing to the close similarity of the chemical vibrators involved in each configuration, the NIR absorption frequencies do not differ markedly, essentially for the *cis*- and *trans*-isomers, as revealed in Fig. 1 representing the spectra of the nearly pure components.

Multivariate calibration methods can be used to establish relations between a spectral mixture data set and the corresponding concentrations for calibration purposes. The use of methods such as principal component regression (PCR) or PLS is of great interest in these cases as these methods are global methods using all the wavenumbers in the spectra (or in a given spectral range) to estimate the properties of interest. In the PLS case, the choice of the principal components is based on the variation of the concentration.

In this work, a multivariate calibration is applied, not only in the NIR region, but also on the MIR and Raman spectra. The principle of the statistical methods for vibrational quantitative analysis is to carry out measurements on calibration standards whose composition has been already determined by an

(a)

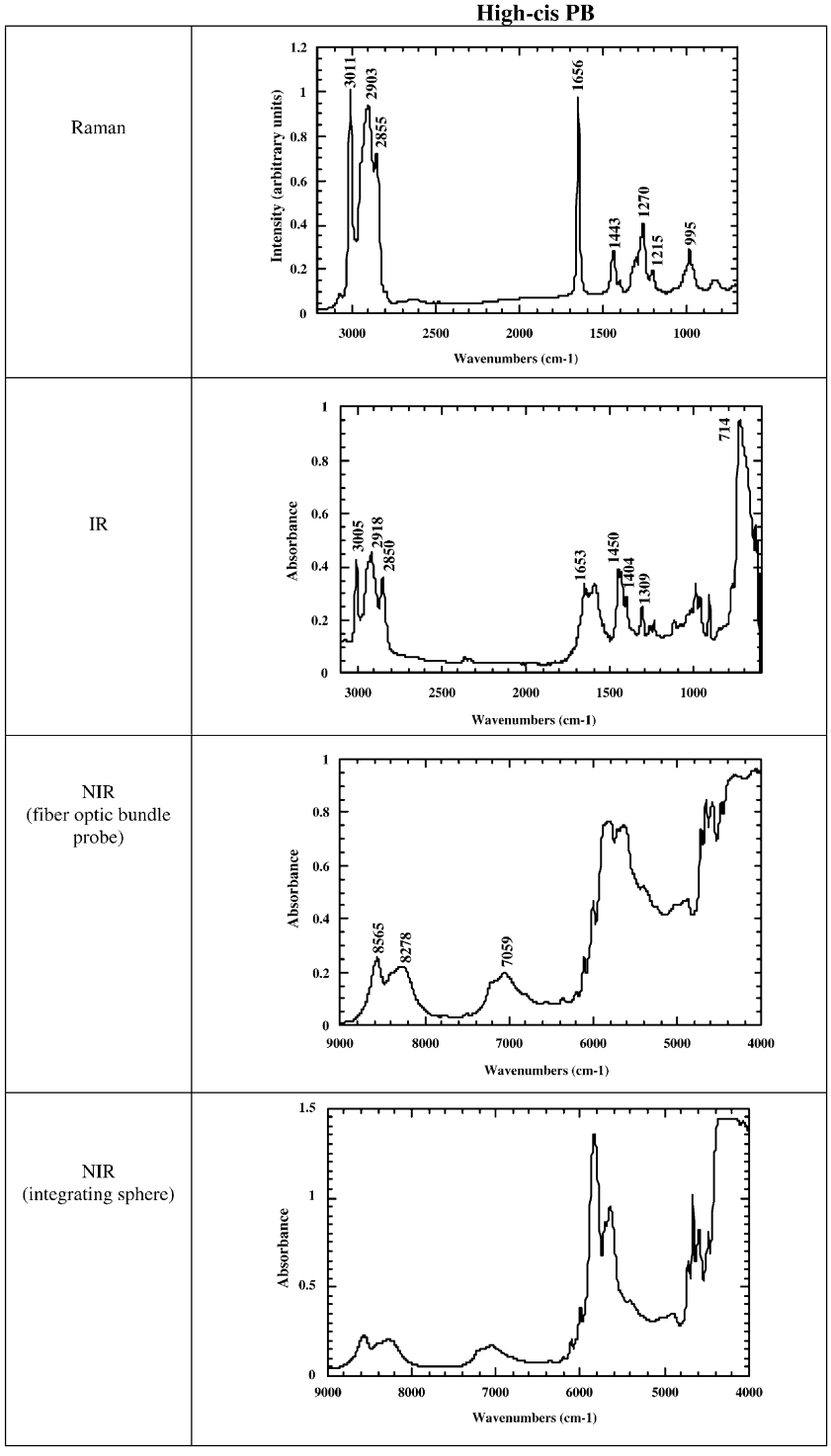

Fig. 1. Vibrational spectra of (a) high-*cis* PB; (b) high-*trans* PB; and (c) high-vinyl PB.

(b)

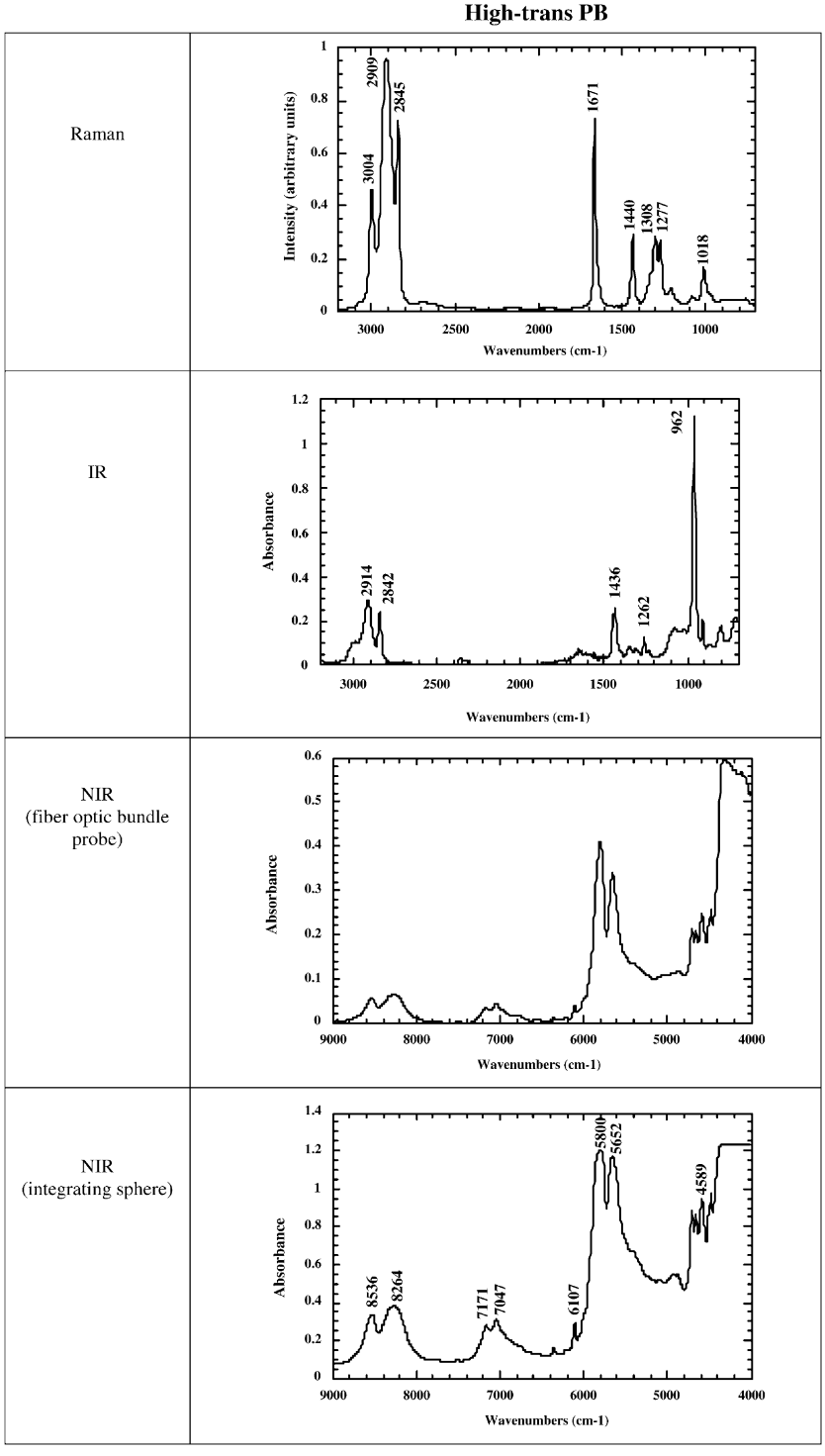

Fig. 1. (*Continued*).

(c) **High-vinyl PB**

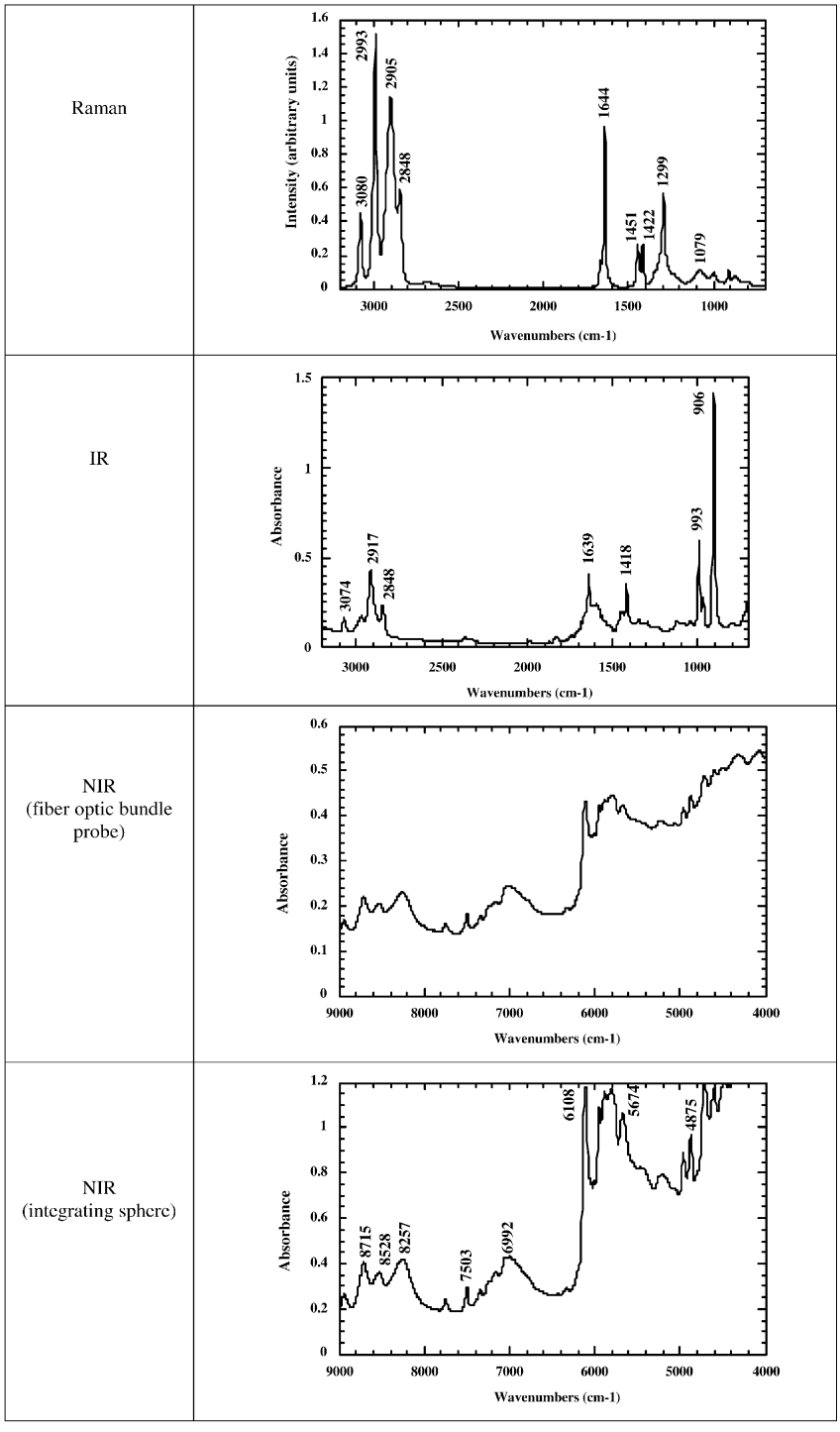

Fig. 1. (*Continued*).

independent traditional chemical or physical method. After setting up a calibration, unknown samples can be predicted on the basis of their spectra, the analysis time being drastically reduced to a few minutes with regard to the traditional time-consuming chemical procedures.

The quality of the models is usually evaluated by several statistical criteria, such as the error of calibration and validation (standard error of prediction, SEP; prediction residual sum of squares, PRESS) [27,28], and also criteria demonstrating the ability of the model to reconstruct unknown spectra (Mahalanobis distance) [29]. The impact of these factors is discussed in the following section.

4. Results and discussion

4.1. Polybutadienes (PB)

As a typical example, spectra obtained in the MIR and NIR as well as Raman spectra of high-*cis*, -*trans* and -vinyl PB are given in Fig. 1. The wavenumbers and the assignments of the fundamental absorption bands of high-*cis*, -*trans* and -vinyl PB, are summarized in Table 1.

The configuration forms display different bands for the stretching vibrations of the CH and CH_2 groups, located in the 2800–3100 cm^{-1} spectral range. Additionally, absorption bands due to the out-of-plane vibrations of the C–H group are characteristic of the substitution patterns around the C=C group, in the MIR spectra of PB. They are located at 732 and 962 cm^{-1}, respectively, for the *cis*- and *trans*-polymers and at 906 and 993 cm^{-1} for the vinyl-polymer.

The Raman spectra are also characterized by the bands associated with the double bond stretching vibration, the bands at 1656, 1670 and 1644 cm^{-1} being representative of, respectively, *cis*-, *trans*- and vinyl-configurations. It is interesting to mention that the ν(C=C) is Raman active for all three structural forms, while that related to the *trans*-configuration is IR inactive due to the presence of a center of symmetry.

Table 1
Wavenumbers and assignments of the main fundamental absorption bands of high-*cis*, -*trans* and -vinyl PBs

Cis		*Trans*		Vinyl		Assignment[a]
Infrared (cm^{-1})	Raman (cm^{-1})	Infrared (cm^{-1})	Raman (cm^{-1})	Infrared (cm^{-1})	Raman (cm^{-1})	
732						CH wag
				906	915	CH_2= wag
		962				CH wag
				993	995	CH wag
			1018			νC–C
1121						νC–C
1240	1215		1212			
1265	1270	1262	1277		1298	CH_2 twist
1309	1312		1308			δ(=CH)
	1355	1352		1347		CH_2 wag
1404	1407					δ(=CH)
				1418	1423	δCH_2=
1435	1443	1436	1440			$\delta_s CH_2$
1450					1451	$\delta_s CH_2$
				1639	1644	νC=C
1653	1656					νC=C
			1671			νC=C
2850	2855	2842	2845	2848	2848	$\nu_s CH_2$
2918	2903	2914	2909	2917	2905	$\nu_a CH_2$
2950	2950					ν(CH=CH)
				2971	2993	$\nu_s CH_2$=
3005	3011		3004			ν(CH=CH)
				3074	3080	$\nu_a CH_2$=

[a] ν: stretching; δ: in-plane bending vibration; wag: out-of-plane C–H bending vibration; s: symmetric; a: antisymmetric.

The NIR spectra are divided into three regions. The region from 4000 to 5000 cm^{-1} contains mainly combination frequencies, arising from C–H stretching frequencies and the other principal modes of vibration, while the region from 5600 to 6100 cm^{-1} contains the first overtones of the aliphatic C–H stretching frequencies. Both regions display differences due essentially to a change in the microstructure of the butadiene phase. The bands located at 4477, 4713 and 6108 cm^{-1} are associated with the vinyl-units. The region from 6500 to 9000 cm^{-1} contains the second overtones of the C–H stretching frequencies.

The NIR spectra obtained with the fiber optic bundle probe in diffuse reflectance mode are very good in the 4500–6500 cm^{-1} region but are rather weak in the 6500–9000 cm^{-1} range. On the other hand, spectra obtained with the integrating sphere are very often saturated in the 4500–6500 cm^{-1} range while giving a signal intensity about 0.5 OD in the 6500–9000 cm^{-1} region. Additionally, due to a larger analyzed surface, the spectra obtained with the integrating sphere are more reproducible than those obtained with the fiber optic bundle probe.

For the models, the investigated frequency ranges in MIR and Raman spectroscopies are 3200–2700, 1800–1500, 6200–5000 and 9000–6500 cm^{-1} in NIR. The latter spectral range was chosen for the quantitative analysis of the NIR spectra since saturated signals often seen between 4000 and 6500 cm^{-1} preclude any data treatment. The 3200–2700 cm^{-1} range has been chosen for the two other techniques since the absorption band associated with the double bond stretching does not appear in the MIR spectrum of the *trans*-unit. Working on the same frequency range in Raman as in MIR allows easier comparison of the results. The purpose of this work is not to obtain the best quantitative model with the three techniques, but to try to give a fair comparison of these techniques including the quantitative results but also the ease of use, sampling conditions and limitations of the methods. In any case, the quantitative results are limited to the precision of the reference method which is a few percent.

It is interesting to mention that it was not possible to apply the HATR technique to the non-antioxidated samples on account of the state of their surface. Non-antioxidized samples surface become very hard with time and the contact with the ATR crystal is then difficult to obtain giving rise to poor IR signal and bad spectra. This is also adding some troubles in the NIR but to a lesser extent. Even if the recent techniques also allow the acquisition of spectra in the MIR and NIR ranges without any sample preparation, the FT-Raman technique appears to be the easiest to use, showing more flexibility for the acquisition of spectra on samples with peculiar surface properties. With the excitation in the NIR (1064 nm for Nd-YAG laser), the laser beam really goes into the sample (estimated penetration is 1 or 2 mm) and allows to study heterogeneous samples if the heterogeneity is smaller than a millimeter.

The PLS algorithm for multivariate calibration in the OPUS/Quant-2 software was applied. It is a PLS1-type algorithm, treating the different components independently. The calibration model is based on a set of 13 different PB samples, containing different amounts of *cis*-, *trans*- and vinyl-units (Table 2). Eight samples with the same combination of components but not protected with antioxidant, were also recorded and added to the calibration list. Finally, 21 samples were available to build up the calibration. The component values of the calibration standards (determined by NMR and MIR analysis) are noted as the 'true values' in the calibration table. The estimated precision of the reference methods is a few absolute percent. A set of 13 different samples is enough to allow a rough comparison of the Quant methods,

Table 2
Molecular characteristics of the PBs

Sample	PB microstructure (%)		
	Cis	*Trans*	Vinyl
PB 1/1 bis[a]	27	67	6
PB 2/2 bis[a]	17	79	4
PB 3/3 bis[a]	29	37	34
PB 4/4 bis[a]	22	24	54
PB 5/5 bis[a]	14	17	69
PB 6/6 bis[a]	10	14	76
PB 7/7 bis[a]	3	13	84
PB 8	79	17	4
PB 9	92	4	4
PB 10/10 bis[a]	40	49	11
PB 11	37	50	13
PB 12	17	28	55
PB 13	11	12	76

[a] Samples prepared without antioxidant.

however if one wants to develop a very precise and accurate method for three components, it would be better to have at least 30 different samples with well known concentrations spread out with a Gaussian repartition around the value of interest for the different properties [30,31].

To establish a quantitative model using the PLS algorithm, it is important to understand and/or visualize the correlation between spectral features and quantitative properties. The first approach is based on the observation of the spectra as described in the previous paragraph. This observation can be completed by the correlogram function given in the software which shows, for each component, the spectral zones with high information content in terms of correlation with the quantitative data.

The quality of the model was improved by performing a data preprocessing of the original spectra (vector normalization) to make them more similar. The vector normalization attenuates variations in sample thickness as well as differences in baseline and/or fluctuations in the source intensity, and has been used for all the models. This pretreatment of the spectra is often the first step for a successful analysis of NIR data [32].

Additionally, it is known [33] that a first-derivative preprocessing of the spectra is often useful in the NIR range to reduce baseline fluctuations and enhance peak separation. For the NIR models, comparison was made of models with and without derivative preprocessing: 'NIR' only includes vector normalization, while 'Fd-NIR' also includes first derivative (Table 3). The use of derivative treatment could be extended to second derivative and/or to IR and Raman data however a lot of our experiments [30,31] demonstrated that going too far in derivative does not improve the results. This is especially true with FT spectroscopy which give very stable spectra in terms of intensities and position of the bands. The trade-off is between signal to noise (*S*/*N*) ratio and peak separation. In the case of IR and Raman, the peaks are rather well separated, the baseline is clean and so vector normalization is sufficient to get good results (MSC does not improve data when the baseline is flat). For NIR spectra, the use of first derivative is a good compromise between *S*/*N* and peak separation. With polymers such as PBs and SBRs, the use of second derivative degrades the results instead of improving them. As already discussed previously, fluorescence

Table 3
PB models

	Raman	HATR	NIR	Fd-NIR
No. of calibration spectra	57	36	54	54
Frequency region (cm^{-1})	2685–3206	2684–3207	6499–9296	6499–9296
No. of factors				
Cis	4	4	4	4
Trans	4	4	5	4
Vinyl	5	4	5	4
R^{2a}				
Cis	99.25	99.57	99.42	99.29
Trans	99.41	99.38	99.30	99.50
Vinyl	99.82	99.85	99.51	99.62
RMSECV[b]				
Cis	2.0	1.75	1.78	1.98
Trans	1.84	1.81	1.85	1.56
Vinyl	1.37	1.24	2.24	1.99
Maximum error/calibration value				
Cis	4.65	4.57	3.06	4.67
Trans	4.22	3.35	4.47	3.27
Vinyl	2.80	2.83	4.09	4.65

[a] R^2: percent of 'interpreted' data.
[b] RMSECV: root mean square error on calibrated values, also called 'prediction error'.

can occur in FT-Raman spectra. The FT-Raman frequency range for calibration was chosen so as to be as free as possible of fluorescence.

The setup of the calibration model is usually done in four steps.

1. The set of spectra collected for the various samples is separated in two sets. Every third spectrum is picked out of the global set to build the 'validation set', while the other spectra are included in the 'calibration set'. The component 'true values' of the validation spectra must strictly be inside the calibration range and statistically homogeneously distributed.
2. The calibration is conducted on the calibration set to build the model by 'cross-validation', following the 'leave-one-out' method: the calibration parameters are adjusted by the software so as to fit with all calibration set spectra except one which is used as a prediction test. The left-out spectrum is thereafter re-included in the calibration set, another one left out and the cycle repeated again, for each spectrum. The predicted value of each of the properties (i.e. *cis*, *trans*, vinyl for the PB samples) of each of the left out spectra with the different models calculated for different numbers of used parameters (typically from 1 to 10) is compared to its corresponding true value to calculate the PRESS. As a calibration result, the plot of the PRESS value versus the number of parameters ('factors') is used for each of the properties to achieve a preliminary choice of the number of factors to be used in the model.
3. The validation set spectra are then used to evaluate the credibility and coherence of the model: using the previously chosen parameter number and values, the properties of the validation spectra are predicted and the SEP calculated; the number of factors previously chosen is compared with the SEP results in order to determine the optimal number for each component. For example, if the PRESS indicates a number of five factors and the SEP 15, it means that the model is good inside the calibration set but unable of any prediction outside it. The number indicated by the SEP should be only slightly higher than the number chosen with the PRESS. When satisfactory, a 'consolidated' calibration is calculated with all the spectra this time, so as to compensate for the restricted number of samples we have.
4. The last step should be an external validation of the model, replaced here by the prediction and repeatability test.

The factors used in the model can be visualized, and the quantity of information they contain can therefore be checked. The *cis*, *trans* and vinyl factors for the PB-series Raman method are shown on Fig. 2 as an example. The method used being a PLS-1, the factors are calculated independently for each component. However, it can be seen on Fig. 2 that they are similar and only used in a different order or with a different sign. As an example, factors are used as *cis* and *trans* (C3 and T4), *cis* and vinyl (C1 and V1) or *trans* and vinyl (T2 and V3), with no or few modifications ($C1 = -V1$, for example). Overall, it can be noted that the factors describing the *cis*- and *trans*-composition are very close together while the vinyl ones are more specific. Similar observations can be made for NIR and MIR calibrations.

Four models were selected: one for Raman, one for HATR, two for NIR (with and without derivative pretreatment). The final results are summarized in Table 3, along with the number of factors used to modelize the set of spectra. The most intuitive number would be three for the PB series, since the only encountered forms are *cis*, *trans* and vinyl. As a matter of fact, higher numbers are revealed by the models, which can be ascribed to band overlaps, impurities, ingredients of formulation or even water. However, we limited the number of factors to five in the models. The differences of number of factors between *cis*, *trans* and vinyl for a given technique can be explained by the fact that one configuration or the other can give rise to more intense peaks or less overlapped ones, thus allowing a good prediction without use of many factors.

The PB 3 sample having the most balanced microstructure was chosen for a calibration–prediction test of the techniques, and the corresponding spectra were kept out of the calibration and validation sets.

Each method was able to explain more than 99% of the variance for every one of the three configurations with about four to five factors (Table 3), which was acceptable referring to the above fixed rules of calibration and prediction.

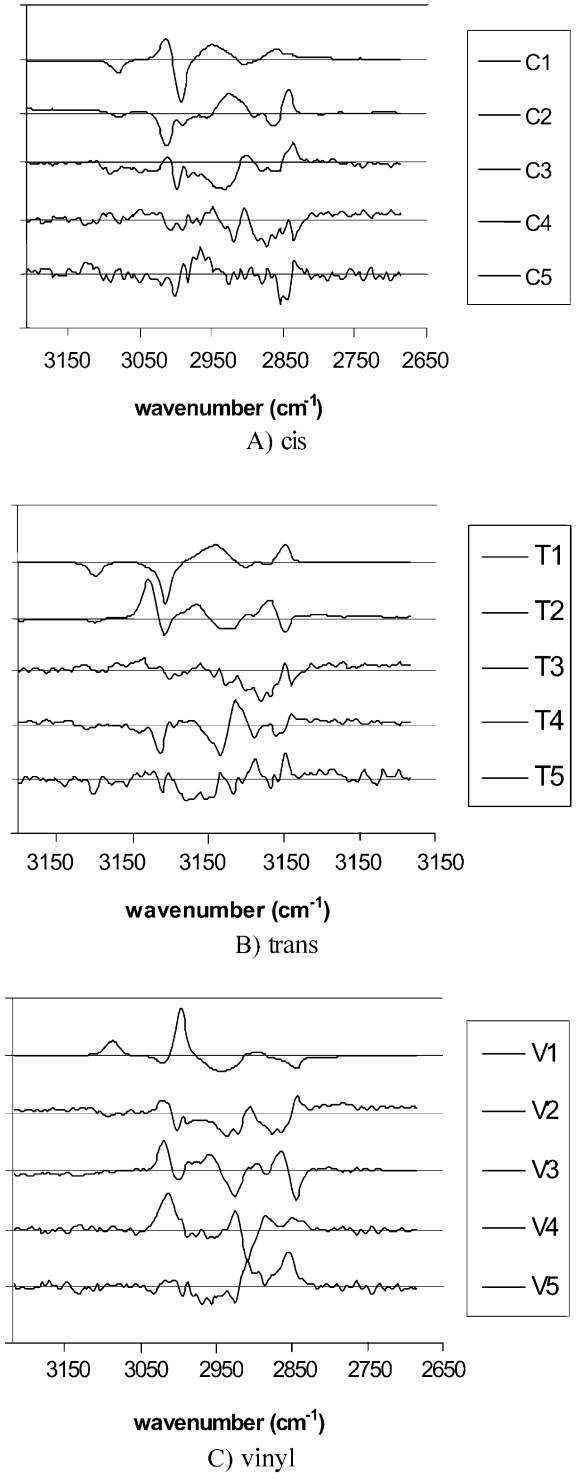

Fig. 2. Raman *cis*, *trans* and vinyl PLS factors.

It has to be mentioned that the calculated calibration model is highly dependent on the accuracy of the 'true values'; the more precise the true values, the more accurate the calibration model, knowing that the calculated model is probably no more precise than the original techniques used to determine the *cis*-, *trans*- and vinyl-proportions (true values) in the samples [30,34].

Our results show that an error of prediction of about 2 absolute% is obtained on the predicted values, with a maximum of 5 absolute% in a few cases. Even in the case of a very small contribution of a given form, all the components are well-predicted by the model (individual calibration results, not shown here).

The NIR methods lead to similar results than the two other techniques for the *cis*- and *trans*-configurations, but are slightly less accurate for the vinyl-calibration (higher RMSECV and maximum error).

Thirty spectra of the PB 3 sample were independently recorded with each spectroscopic technique, and the prediction and repeatability results were then quickly obtained by treatment of the PB 3 spectra with the methods described above.

As seen in Table 4, the four models (Raman, HATR, NIR and first-derivative NIR) gave similar results, thus inter-validating each other. The expected values (29% *cis*, 37% *trans* and 34% vinyl) are obtained within ±2 absolute% for *cis*, ±3% for *trans* and ±4% for vinyl. The *cis*-prediction results obtained for the Raman spectra are presented in Fig. 3. The NIR methods gave the most accurate results for the overall prediction. The derivative pretreatment improves the accuracy of the prediction, but leads to higher Mahalanobis distances (just inside the limit for the vinyl-prediction, and signaled as possible outlier for the *cis*-prediction), accounting for a bad spectrum reconstruction. This probably explains the slight decrease observed in the repeatability values for the derivative method.

Beside the problems linked to pressure adjustment, the HATR technique leads to less precise results, essentially for the *trans* and vinyl forms. It would be interesting to test the new diamond ATR accessories (we did not have one available) to see if it allows to solve the pressure problem and improves the overall precision of the MIR method.

Despite the higher variance in the repeatability results due mainly to the stability of the laser, the

Table 4
PB repeatability results

	Cis				*Trans*				Vinyl			
	Prediction	σ^2	Mahalanobis	Limit	Prediction	σ^2	Mahalanobis	Limit	Prediction	σ^2	Mahalanobis	Limit
Raman	28	5.0E–2	0.05	0.14	40	5.0E–2	0.06	0.14	33	1.5E–2	0.06	0.18
HATR	29	1.2E–2	0.06	0.22	33	5.3E–2	0.09	0.22	37	5.3E–3	0.10	0.22
NIR	31	2.2E–3	0.09	0.15	39	1.2E–3	0.03	0.19	30	2.2E–3	0.04	0.19
Fd-NIR	30	2.4E–3	0.16	0.15	36	9.4E–3	0.01	0.15	33	7.4E–3	0.14	0.15
True values	29				37				34			

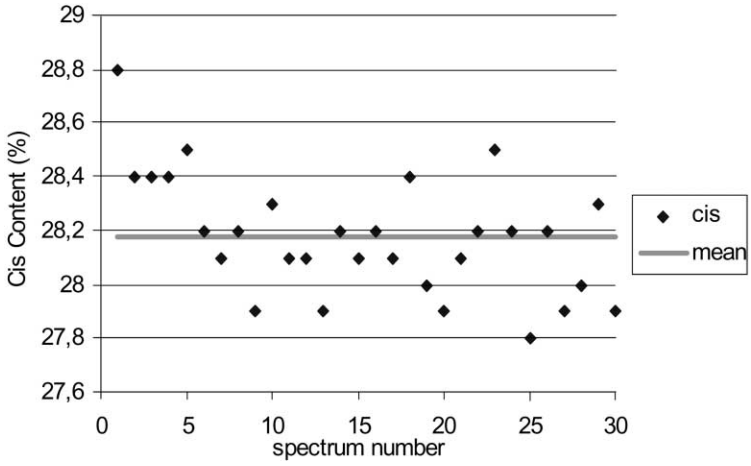

Fig. 3. *Cis* Raman repeatability results.

FT-Raman technique is less sensitive to the sample state and thus gives access to a larger range of calibration spectra, resulting in an overall good prediction of the microstructure.

4.2. Styrene–butadiene rubbers (SBR)

For the analysis of the SBR copolymers, nine samples containing different amounts of *cis*-, *trans*-, vinyl- and styrene-units (Table 5) were used for the calibration. The spectra of pure polystyrene as well as those of a styrene–butadiene copolymer (SBR1) used as a typical example, are shown in Fig. 4.

An attempt to predict the SBR copolymer composition using the models previously developed for the PBs gave incoherent results: the models were unable to correctly predict the *cis*, *trans* and vinyl amounts in the SBRs, the contribution of the styrene being added either to the *cis*, *trans* or vinyl part of the spectra. This led to develop a specific model for the SBRs.

The model obtained with the only few samples available gave satisfactory results (shown in Table 6)

Table 5
Molecular characteristics of the styrene–butadiene copolymers

Sample	Butadiene microstructure (%)			Styrene (wt.%)
	Cis	*Trans*	Vinyl	
SBR 1	9	55	13	23
SBR 2	18	25	33	24
SBR 3	21	35	18	26
SBR 4	13	17	45	25
SBR 5	31	41	10	18
SBR 6	29	39	8	24
SBR 7	23	33	17	27
SBR 8	18	31	24	27
SBR 9	14	30	15	41

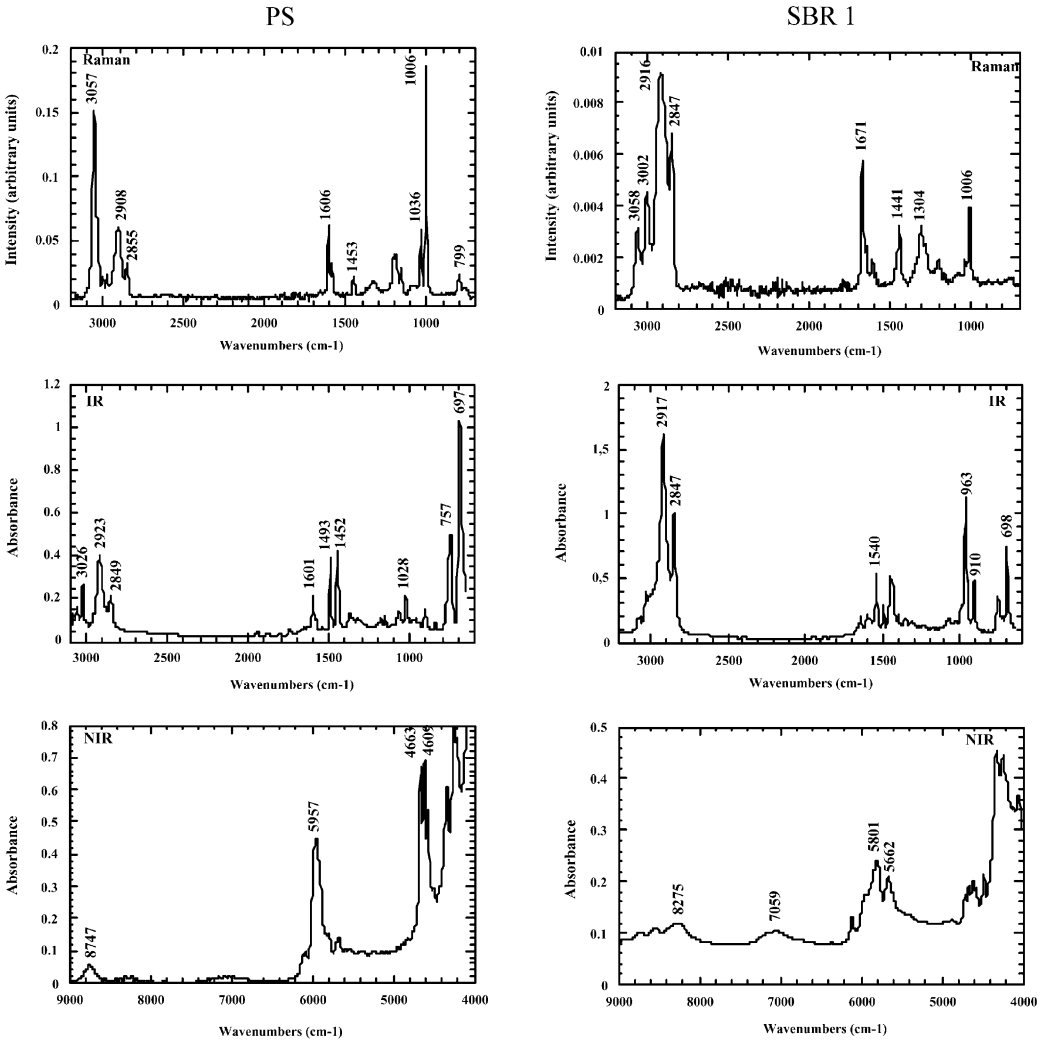

Fig. 4. Polystyrene and styrene–butadiene copolymer (SBR1) vibrational spectra.

with only some discrepancies in the *cis*- and *trans*-predictions in Raman. The prediction results, conducted on an independent set of thirty spectra of the SBR 7 sample, are given in the 'SBR-only' part of Table 7.

An alternative solution, leading to better results, was to add the SBR spectra and a fourth component (styrene) in the PB models. The numbers of factors were re-adjusted, following the same methodology as above, allowing up to eight factors. The characteristics of the modified models are given in Table 8.

Each one of the four methods gave similar results for the R^2, allowing calibration of more than 99% of the data (99.05–99.78%). It is interesting to notice that a significant number of possible outliers are reported, showing that the additional spectra have reduced the calibration error tolerance of the models. Another remarkable point is that the maximum error values for the *cis*-, *trans*- and vinyl-components always are obtained on PB samples, while the maximum error on the styrene calibration arises from SBR samples. This result is rather counter-intuitive: the SBRs should

Table 6
SBR models[a]

	RAM	HATR	NIR	Fd-NIR
No. of calibration spectra	27	27	27	27
Frequency region (cm^{-1})	2797–3150	2796–3151	6499–9296	6499–9296
No. of factors				
Cis	4	6	6	5
Trans	4	5	5	4
Vinyl	4	4	5	5
Styrene	6	6	6	7
RMSECV				
Cis	1.59	0.50	0.41	0.29
Trans	1.17	0.28	0.40	0.36
Vinyl	0.53	0.16	0.23	0.35
Styrene	0.53	0.28	0.20	0.20

[a] RMSECV: root mean square error on calibrated values, also called 'prediction error'.

instead have given smaller errors on the styrene compound than the PBs would normally have and vice versa.

Once more, the Raman method seems especially interesting since it was able to achieve those results with six factors or less for each component, while the other methods needed all eight factors for at least one component. This can be explained by the fact the styrene bands are very intense and sharper in Raman than in MIR or NIR. Derivating the spectra in NIR required less factors and led to a better prediction of the styrene component.

In the next step (external validation) it was important to check that the PB predictive ability of the models was not weakened by the addition of the SBR spectra to the PB sample set. As seen in the 'PB + SBR' part of Table 7, the resulting models are even better than without the SBRs: the prediction error on the PB 3 repeatability spectra is lower than before for each of the three first components, and the absence of styrene is generally well predicted (0–1% predicted), except for the HATR method (4%). The HATR method was thus once again the worst of the four, the three other being this time quite equivalent. The Fd-NIR method being the only one to predict 0% styrene should be preferred, followed by the Raman method because of its comfortable Mahalanobis distance results (good reconstitution of the spectra).

The prediction and repeatability results for the SBRs were obtained on the independent set of 30 spectra of the SBR 7 sample. As can be seen in the 'SBR + PB' part of Table 7, every one of the four methods gives good results for this series of prediction. Even if the Raman method was less accurate in this case (maximum error 2.6 absolute%, average error 1.7 absolute%), this method gave the smallest Mahalanobis distances. Those of the NIR method are the greatest, with moreover 2.8 absolute% error on the vinyl-prediction, leading to consider this method as the worst one. On the other hand, the Fd-NIR and HATR methods seemed equivalent, the Fd-NIR one being more accurate on the styrene prediction and slightly less on the vinyl, with Mahalanobis distances very close to the HATR ones in any case.

It must be emphasized that the PB 8 and PB 9 spectra were almost essential for the accuracy of the PB methods, allowing a good discrimination between the *cis*- and *trans*-configurations because of their high *trans* content. In the SBR case, the addition of spectra of pure styrene was catastrophic for the models, the inhomogeneously distributed data being oversensitive, with a cluster of points between 18 and 41% and a single one at 100%. Therefore no pure styrene spectrum was included in the data set.

These facts point out the usefulness of samples with high amounts of a given component. However, taking a polymer with a pure configuration does not automatically improve the robustness of the model, because the concentrations of the various components need to be homogeneously distributed.

Table 7
Prediction and repeatability results[a]

		Cis				*Trans*				Vinyl				Styrene			
		Prediction	σ^2	Mahalanobis	Limit	Prediction	σ^2	Mahalanobis	Limit	Prediction	σ^2	Mahalanobis	Limit	Prediction	σ^2	Mahalanobis	Limit
PB-only	Raman	28	5.0E–2	0.05	0.14	40	5.0E–2	0.06	0.14	33	1.5E–2	0.06	0.18	N/A	N/A	N/A	N/A
	HATR	29	1.2E–2	0.06	0.22	33	5.3E–2	0.09	0.22	37	5.3E–3	0.10	0.22	N/A	N/A	N/A	N/A
	NIR	31	2.2E–3	0.09	0.15	39	1.2E–3	0.03	0.19	30	2.2E–3	0.04	0.19	N/A	N/A	N/A	N/A
	Fd-NIR	30	2.4E–3	0.16	0.15	36	9.4E–3	0.01	0.15	33	7.4E–3	0.14	0.15	N/A	N/A	N/A	N/A
PB + SBR	Raman	28	5.8E–2	0.04	0.12	39	4.0E–2	0.05	0.12	32	1.3E–2	0.04	0.14	1	6.0E–3	0.04	0.14
	HATR	30	3.3E–4	0.04	0.20	34	1.1E–1	0.06	0.23	35	7.2E–2	0.17	0.27	4	2.6E–2	0.09	0.23
	NIR	30	2.2E–3	0.09	0.17	38	9.3E–4	0.06	0.20	32	1.7E–3	0.12	0.20	1	1.4E–3	0.12	0.20
	Fd-NIR	29	3.0E–3	0.03	0.12	37	6.5E–3	0.05	0.15	32	4.1E–3	0.17	0.20	0	1.9E–3	0.12	0.17
True values		29				37				34				0			
SBR + PB	Raman	21.0	4.4E–2	0.05	0.12	35.5	1.6E–1	0.03	0.12	18.4	7.8E–2	0.03	0.14	25.3	5.9E–2	0.03	0.14
	HATR	21.1	2.3E–3	0.07	0.20	32.7	2.9E–2	0.07	0.23	17.4	6.2E–2	0.08	0.27	29.0	9.4E–3	0.05	0.23
	NIR	20.7	0.0	0.04	0.17	32.5	2.6E–3	0.11	0.20	20.3	2.4E–3	0.12	0.20	26.4	9.3E–4	0.08	0.20
	Fd-NIR	21.2	2.5E–3	0.06	0.12	32.4	3.3E–3	0.09	0.15	19.6	1.0E–2	0.08	0.20	26.5	2.7E–3	0.07	0.17
SBR-only	Raman	19.4	6.8E–2	0.01	0.30	36.0	9.7E–2	0.01	0.30	18.1	3.8E–2	0.02	0.30	27.0	2.8E–2	0.12	0.44
	HATR	21.7	4.9E–2	0.25	0.44	33.7	3.0E–2	0.14	0.37	17.0	1.0E–3	0.05	0.30	27.0	1.0E–2	0.28	0.44
	NIR	22.4	2.2E–3	0.29	0.44	32.9	8.8E–13	0.06	0.37	17.0	9.3E–4	0.07	0.37	26.6	2.6E–3	0.12	0.44
	Fd-NIR	23.0	6.9E–4	0.21	0.37	32.3	2.4E–3	0.04	0.30	17.7	1.0E–3	0.26	0.37	27.1	1.7E–3	0.23	0.52
True values		22.6				32.9				17.5				27.0			

[a] N/A: no such component in the 'PB-only' models.

Table 8
PB + SBR models[a]

	RAM	HATR	NIR	Fd-NIR
No. of calibration spectra	84	60	81	81
Frequency region (cm^{-1})	2685–3207	2683–3207	6499–9296	6499–9296
No. of factors				
Cis	5	6	7	5
Trans	5	7	8	6
Vinyl	6	8	8	8
Styrene	6	7	8	7
RMSECV				
Cis	1.81	1.58	1.51	1.81
Trans	1.95	1.05	1.85	1.34
Vinyl	1.45	1.65	1.72	1.50
Styrene	1.06	1.09	0.61	0.62

[a] RMSECV: root mean square error on calibrated values, also called 'prediction error'.

5. Conclusion

This paper is the first one of a series using vibrational spectroscopy to investigate polymer properties. It is specially devoted to the determination of a microstructure and a polymer composition by means of chemometric treatments applied to MIR and NIR data as well as to Raman measurements obtained without any sample preparation. A critical assessment of these spectroscopic techniques is also reported. In each case, it appears that the Raman method is particularly recommended for in line or rapid study of samples as they come since it is less sensitive to the state of the investigated samples. On the other hand, NIR is also very interesting because it does not require a lot of sample preparation (a flat surface of a few squared centimeters is enough) and it gives very stable results over time.

Even if we got satisfactory results in terms of precision and accuracy for each of the techniques, a full calibration set would be needed to really be used in a production area either fulfilling the calibration with samples of composition from 0 to 100% of each of the components (*cis*, *trans*, vinyl, styrene) if one wants to analyze all kinds of PB and SBR rubbers or selecting a narrower range of compositions around a given aim if one wants to control a production stream.

In a forthcoming paper, a more detailed band assignment of the NIR spectral region will be given by applying a two-dimensional correlation analysis which consists of interpreting the NIR peaks based over a second dimension spectroscopy (MIR and/or Raman).

References

[1] R.M. Bly, P.E. Kiener, B.A. Fries, Anal. Chem. 38 (1966) 217.
[2] W.H. Greive, D.D. Doepken, Polym. Eng. Sci. 1 (1968) 19.
[3] T. Takeuchi, S. Tsuge, Y. Sugimura, Anal. Chem. 41 (1969) 184.
[4] V.L. Kofman, M.P. Teterina, G.N. Bondarenko, Polym. Sci. USSR 21 (1980) 1676.
[5] R. Mao, M. Huglin, T.P. Davis, Eur. Polym. J. 29 (1993) 475.
[6] R.S. Silas, J. Yates, V. Thorton, Anal. Chem. 31 (1959) 529.
[7] D.L. Snavely, C. Angevine, J. Polym. Sci. A: Polym. Chem. 34 (1996) 1669.
[8] R.G.J. Miller, H.A. Willis, J. Appl. Chem. 6 (1956) 385.
[9] J.L. Binder, J. Polym. Sci. A 3 (1965) 1597.
[10] S.W. Cornell, J.L. Koenig, Macromolecules 2 (1969) 540.
[11] H.J. Sloane, R. Bramston-Cook, Appl. Spectrosc. 27 (1973) 217.
[12] S. Poshyachinda, H.G.M. Edwards, A.F. Johnson, Polymer 32 (1991) 338.
[13] H.J. Harwood, Rubber Chem. Technol. 55 (1982) 769.
[14] G. Van der Velden, C. Didden, T. Veermans, J. Beulen, Macromolecules 20 (1987) 1252.
[15] G.P.M. Van der Velden, L.J. Fetters, Macromolecules 23 (1990) 2470.
[16] J.A. Frankland, H.G. Edwards, A.F. Johnson, I.R. Lewis, S. Poshyachinda, Spectrochim. Acta 47A (1991) 1511.
[17] H.W. Siesler, Makromol. Chem., Macromol. Symp. 52 (1991) 113.

[18] K.A. Bunding Lee, Appl. Spectrosc. Rev. 28 (1993) 231.
[19] T. Buffeteau, B. Desbat, L. Bokobza, Polymer 36 (1995) 4339.
[20] D. Fischer, K.-J. Eichhorn, Anal. Magazine 26 (1998) M58.
[21] T. Hirschfeld, B. Chase, Appl. Spectrosc. 40 (1986) 133.
[22] P. Hendra, H. Mould, Int. Lab. 34 (1988).
[23] W. Kaye, Spectrochim. Acta 6 (1954) 257.
[24] K.B. Whetsel, Appl. Spectrosc. Rev. 2 (1968) 1.
[25] J.J. Workman Jr., Appl. Spectrosc. Rev. 31 (1996) 251.
[26] L. Bokobza, J. Near Infrared Spectrosc. 6 (1998) 3.
[27] P. Geladi, B.R. Kowalski, Anal. Chem. Acta 19 (1986) 185.
[28] J.J. Berzas Nevado, C. Guiberteau, A.M. Cabanillas, C. Salcedo, Analysis 22 (1994) 5.
[29] H. Martens, T. Næs, Multivariate Calibration, Wiley, Chichester, 1989.
[30] R. Cinier, J. Guilment, Vibrational Spectrosc. 11 (1996) 51–59.
[31] R. Cinier, J. Guilment, J. Near Infrared Spectrosc. 6 (1998) 291.
[32] J. Sun, J. Chemometrics 11 (1997) 525.
[33] M.J. Adams (Ed.), Chemometrics in Analytical Spectroscopy, The Royal Society of Chemistry, 1995.
[34] R. DiFoggio, Appl. Spectrosc. 54 (2000) 3.